ADVANCED BIOLOGY
www.advanced-bio.com

Combination Therapy With CD147-Targeted Nanoparticles Carrying Phenformin Decreases Lung Cancer Growth

*Andreia Pereira-Nunes, Helena Ferreira, Sara Abreu, Marta Guedes, Nuno M. Neves, Fátima Baltazar, and Sara Granja**

Lung cancer is one of the most fatal cancers worldwide. Resistance to conventional therapies remains a hindrance to patient treatment. Therefore, the development of more effective anti-cancer therapeutic strategies is imperative. Solid tumors exhibit a hyperglycolytic phenotype, leading to enhanced lactate production; and, consequently, its extrusion to the tumor microenvironment. Previous data reveals that inhibition of CD147, the chaperone of lactate transporters (MCTs), decreases lactate export in lung cancer cells and sensitizes them to phenformin, leading to a drastic decrease in cell growth. In this study, the development of anti-CD147 targeted liposomes (LUVs) carrying phenformin is envisioned, and their efficacy is evaluated to eliminate lung cancer cells. Herein, the therapeutic effect of free phenformin and anti-CD147 antibody, as well as the efficacy of anti-CD147 LUVs carrying phenformin on A549, H292, and PC-9 cell growth, metabolism, and invasion, are evaluated. Data reveals that phenformin decreases 2D and 3D-cancer cell growth and that the anti-CD147 antibody reduces cell invasion. Importantly, anti-CD147 LUVs carrying phenformin are internalized by cancer cells and impaired lung cancer cell growth in vitro and in vivo. Overall, these results provide evidence for the effectiveness of anti-CD147 LUVs carrying phenformin in compromising lung cancer cell aggressiveness.

1. Introduction

Lung cancer remains the most commonly diagnosed and most fatal cancer worldwide. In 2020, GLOBOCAN estimated 221 million new lung cancer cases with 1.80 million deaths per year.[1] Surgical resection, chemotherapy, and/or radiotherapy are the standard of care treatments for localized and metastatic lung tumors. The unsatisfactory therapeutic specificity and efficiency of these therapies, together with the severe off-target effects, led to the emergence of targeted therapies and immunotherapies.[2] Despite significant improvements in clinical outcomes, long-term disease control only occurs in a minority of patients. Lung cancer represents a high burden for society and the increasing number of new cases (3.50 million) and related deaths (2.94 million) projected for 2040 urges the need for new effective therapeutic options.[1] Therefore, the development of novel therapeutic strategies is imperative to improve site-specific drug delivery, enhance drug load in tumors, and diminish treatment-associated side effects.[3]

Liposomal drug delivery systems have been extensively exploited to overcome or at least minimize the drawbacks of conventional cancer therapies. Interestingly, a number of liposomal formulations has been approved or is undergoing clinical trials for the treatment of various tumors, including lung cancer. Indeed, the non-toxic, biodegradable, and biocompatible nature of liposomes makes them excellent therapeutic carriers.[4] Liposomes are nanosized lipid bilayered vesicles that can entrap water-soluble and lipid-soluble drugs in the aqueous central part and in the lamellae, respectively.[5] They can be surface modified with polyethylene glycol (PEG)-like polymers to augment their

A. Pereira-Nunes, S. Abreu, F. Baltazar, S. Granja
Life and Health Sciences Research Institute (ICVS)
School of Medicine
University of Minho
Campus de Gualtar, 4710-057 Braga, Portugal
E-mail: saragranja@med.uminho.pt

A. Pereira-Nunes, H. Ferreira, S. Abreu, M. Guedes, N. M. Neves, F. Baltazar, S. Granja
ICVS/3B's-PT Government Associate Laboratory
Guimarães, 4710-057 Braga, Portugal

H. Ferreira, M. Guedes, N. M. Neves
3B's Research Group
I3Bs – Research Institute on Biomaterials
Biodegradables and Biomimetics
University of Minho
Headquarters of the European Institute of Excellence on Tissue Engineering and Regenerative Medicine
AvePark, Parque de Ciência e Tecnologia, Zona Industrial da Gandra, Barco, 4805-017 Guimarães, Portugal

S. Granja
Department of Pathological
Cytological and Thanatological Anatomy
ESS|P.PORTO
4200-072 Porto, Portugal

The ORCID identification number(s) for the author(s) of this article can be found under https://doi.org/10.1002/adbi.202300080

DOI: 10.1002/adbi.202300080

stability, reduce their uptake by the mononuclear phagocytic system, and prolong their time in circulation.[6] Moreover, liposomes can be conjugated with targeting moieties, such as antibodies, to specifically target tumor cells expressing the corresponding receptors; and therefore, the controlled and sustained release of the encapsulated drugs will occur at the diseased site.[7]

CD147 (also known as basigin of EMMPRIN) is a transmembrane glycoprotein highly expressed on the surface of tumor cells.[8] CD147 plays pleotropic roles in cancer: it stimulates the production of matrix metalloproteinases (MMPs) and vascular endothelial growth factor (VEGF) to promote tumor invasion and angiogenesis; it stabilizes the formation of multiprotein complexes containing drug transporters that drive multidrug resistance; and it regulates the expression and activity of monocarboxylate transporters (MCTs) 1/4 to export proton-coupled lactate derived from glycolysis, acidifying the tumor microenvironment.[9–11] Moreover, this glycolytic–acidic resistant phenotype of tumor cells is further increased under hypoxic conditions due to the upregulation of CD147, MCT1, and MCT4. In fact, it was reported that MCT4 and CD147 are transcriptionally activated by HIF-1α in response to hypoxia, whereas MCT1 expression is increased in a HIF-1α independent way.[12–14] Thus, CD147 has been identified as an attractive target for cancer therapy.

Previous results from our group showed that CD147 KO lung cancer cell lines exhibited a lower expression and activity of MCT1 and MCT4. Hence, these cells showed a decrease in lactate export, a decreased glycolysis activity, and a higher respiratory rate. This study also demonstrated that CD147 plays a crucial role in the control of lactate export and glycolysis rate in lung cancer cells, and targeting this protein sensitizes tumor cells to mitochondrial inhibitors, namely phenformin.[15]

Phenformin is a biguanide drug used clinically for the treatment of type II diabetes.[16] However, its association with lactic acidosis prompted the withdrawal of phenformin from the market.[17] Phenformin-associated lactic acidosis is linked to its lipophilic structure that enables phenformin to cross biological membranes through passive diffusion, reaching/accumulating in the mitochondrial matrix, and inhibiting the respiratory complex I.[18–20] Nonetheless, recent studies have demonstrated that phenformin has potent anti-neoplastic effects on several types of cancer. Indeed, phenformin presents ability to inhibit cell proliferation, invasion and angiogenesis, induce cell cycle arrest and cell apoptosis, and more importantly, decrease tumor growth and metastasis.[19,21] In this regard, phenformin can be a promising anti-cancer agent for lung and other cancers.[22,23]

Based on the above observations, we hypothesized that formulating phenformin inside liposomes would enhance the anticancer therapeutic efficacy of phenformin at lower doses and reduce its side effects. Furthermore, by coating these liposomes with an anti-CD147 monoclonal antibody, we selectively targeted cancer cells, reduced the systemic effects of phenformin, and compromised CD147 function. Hence, this work envisioned the development of CD147-targeted liposomes carrying phenformin and the evaluation of their anticancer potential, which was assessed using in vitro and in vivo lung cancer models.

2. Results

2.1. CD147 Expression in Human Lung Cancer Cell Lines

We first investigated the expression of CD147 and lactate transporters MCT1/4 in A549 and H292 lung cancer cells in normoxia and hypoxia conditions by Western blot and immunofluorescence. The results showed that all proteins are expressed in the cytoplasm and at the plasma membrane of A549 WT and H292 cells; whereas in A549 CD147KO cells, the expression of MCT1/MCT4 and CD147 was negligible. Therefore, the KO cells were used as negative control. As expected, higher expression levels of MCT1 and MCT4 were observed under hypoxia compared to normoxia (**Figure 1**).

2.2. Cytotoxicity of Free Phenformin in Lung Cancer Cells

Before incorporating phenformin into functionalized liposomes with anti-CD147 Ab, preliminary studies were performed to assess the sensitivity of lung cancer cells to phenformin and to assess the anti-CD147 Ab specificity and capacity to inhibit CD147 function.

First, we evaluated the effect of free phenformin in the viability of A549, H292, and PC-9 lung cancer cells by sulphorhodamine B assay. All cell lines showed high sensitivity to phenformin in a dose-dependent manner, with H292 cells being slightly more sensitive than A549 and PC-9 cells (**Figure 2**a; Figure S1a, Supporting Information). Furthermore, and to validate the anticancer effect of phenformin, we tested its impact on 3D-spheroid tumor models because they better reflect the in vivo microenvironment in terms of nutrients, oxygen gradients, and cell–cell interactions.[24] In accordance with the results observed in Figure 2B, phenformin was able to significantly decrease A549 and H292-tumor spheroid growth.

2.3. Effect of Anti-CD147 Ab on Lung Cancer Metabolism and Invasion

Next, we adressed the specificity of the selected anti-CD147 Ab (i.e., Leaf Purified Anti-Human CD147 antibody) to target CD147 on lung cancer cells. For that purpose, we incubated A549 WT and CD147KO cells with the neutralizing antibody overnight; and then, the expression of CD147 was analyzed by immunofluorescence. The results revealed that the anti-CD147 Ab was specific for CD147 because it recognized this protein in CD147-expressing cells and not in CD147KO cells (**Figure 3**a). We further selected a range of antibody concentrations that would not compromise cell viability by toxicity. Thus, increasing doses of an isotype control antibody were tested in A549 WT, A549 CD147KO, and H292 cells and no cytotoxic effects were observed between 10 and 300 ng mL^{-1} (Figure 3b). Therefore, we next incubated these lung cancer cells with the anti-CD147 Ab, at non-toxic concentrations, to study its effect on cell viability.

As shown in Figure 3c, the anti-CD147 Ab did not compromise cell viability in all cell lines. Although no effects on cell

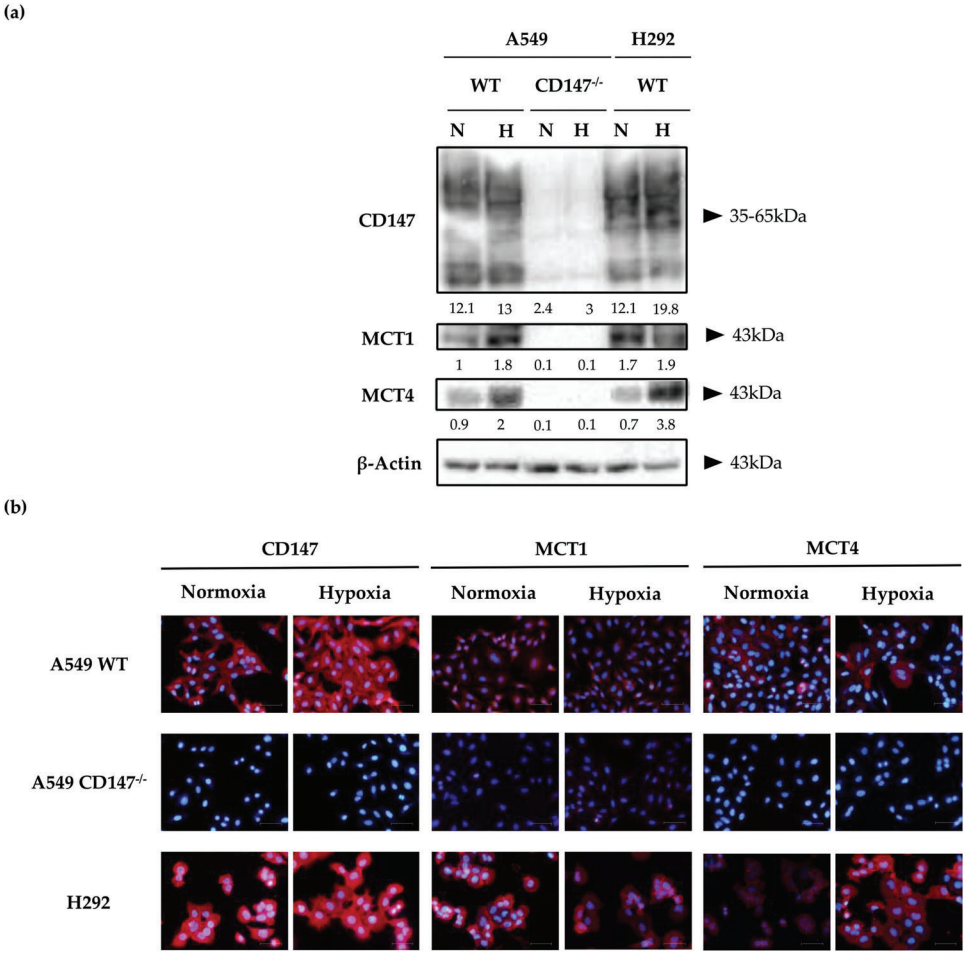

Figure 1. Protein levels and cellular localization of CD147, MCT1, and MCT4 in lung cancer cell lines. a) Western blot and b) immunofluorescence staining of CD147 and MCT1/4 in A549 WT, A549 CD147KO ($^{-/-}$), and H292 cells exposed to normoxia (N) or hypoxia (H) for 24 h. The numbers below indicate the protein quantification of each blot normalized to β-Actin. 200× magnification (DAPI, blue – nuclei; Red – CD147, MCT1, or MCT4); Scale bar: 50 μm.

viability were found, we quantified the extracellular lactate levels in antibody-treated cancer cells in order to understand whether anti-CD147 Ab could disrupt CD147 function as MCT1 and MCT4 chaperone; and consequently, compromise lactate export. We verified that none of the concentrations tested were able to decrease the lactate release from lung cancer cells (**Figure 4**a), suggesting that perhaps, this antibody could be acting in another Ig-domain epitope of CD147 that would not interrupt its interaction with MCTs.

Previous studies reported that mono- and polyclonal antibodies against CD147 were able to decrease MMP secretion; and consequently, cancer cell invasion. Therefore, we went to explore the impact of anti-CD147 Ab on CD147 activity as a MMP-inducer. For that purpose, we generated A549 WT, A549 CD147KO, and H292 3D-cell spheroids; and then, incubated them on matrigel containing the anti-CD147 Ab. This antibody demonstrated to be able to inhibit the invasiveness capacity of A549 WT cells contrarily to A549 CD147KO cells. Although no significant results were found for H292 cells, a trend decrease was noted on cell invasion upon anti-CD147 Ab treatment (Figure 4b).

2.4. LUVs Size Distribution and Zeta-Potential

LUVs incorporating or not incorporating phenformin were characterized in terms of size, PDI, and zeta-potential. **Table 1** presents the hydrodynamic diameter based on the intensity size distribution (Figure S1b, Supporting Information) and shows that LUVs incorporating or not incorporating phenformin presented similar sizes. The size was 153.9 + 5.3 nm for empty LUVs and 158.4 + 8.1 nm for liposomes encapsulating phenformin. The PDI values were lower than 0.2, indicating the homogeneity of the LUVs populations in terms of size. Zeta-potential measurements revealed that LUVs presented a negative surface charge (−23.6 ± 3.7 mV and −28.5 ± 4.3 mV for empty liposomes or with phenformin in their composition).

2.5. Anti-Cancer Activity of LUVs Carrying Phenformin

As previously mentioned, the lung cancer cell lines used in this study were sensitive to phenformin. However, it was shown that

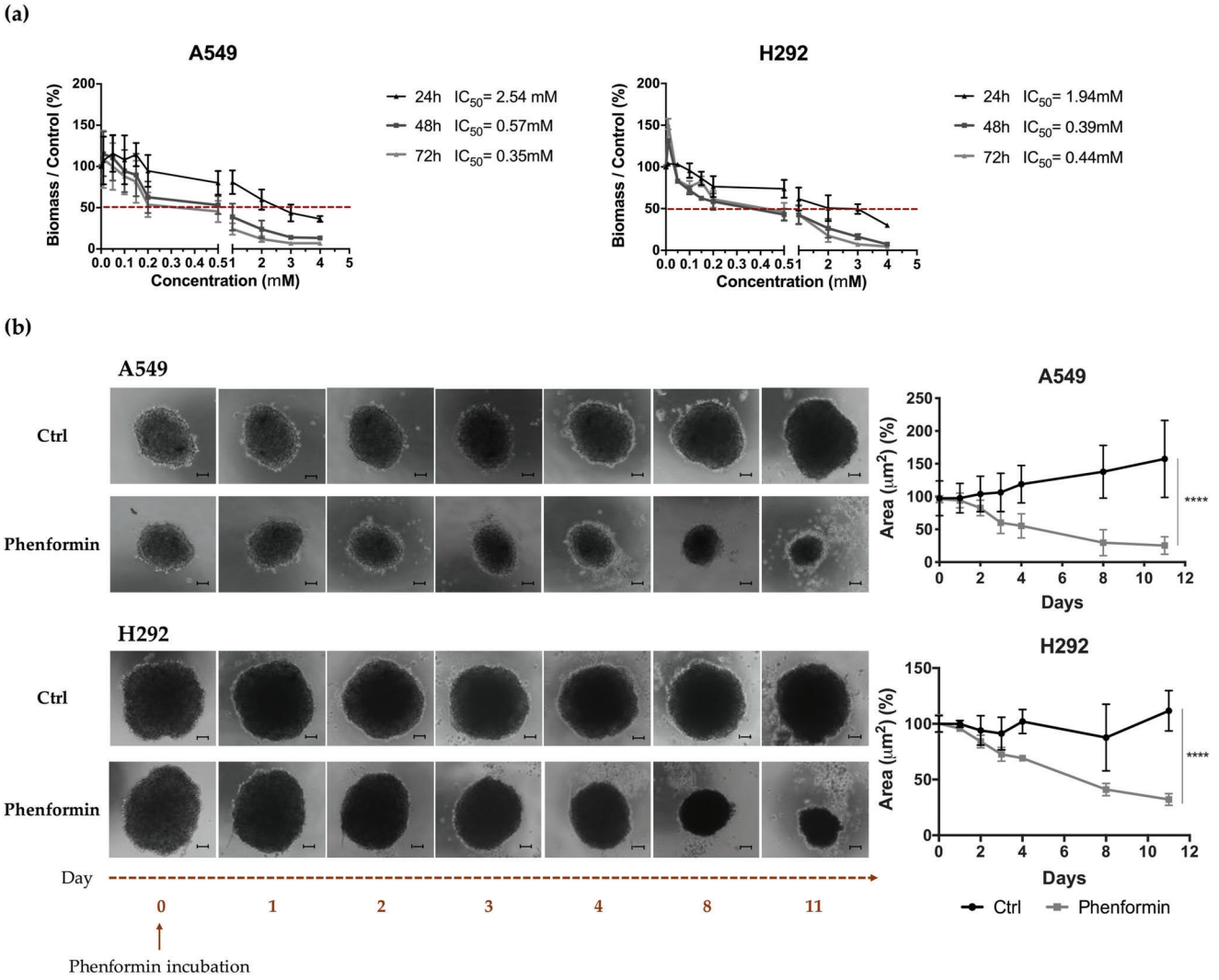

Figure 2. Effect of phenformin in 2D and 3D-lung cancer cell growth. a) A549 and H292 cell viability was assessed by SRB assay at 24, 48, and 72 h incubation with increasing concentrations of phenformin (0.01–4 mM). Results were normalized to the control (DMEM 1% FBS). b) 3D-spheroid growth was analyzed after treatment with DMEM 10% FBS (Ctrl), 2 or 1 mM of phenformin ($n_{spheroids} = 8$ per condition). Images were taken at 40× magnification using the Olympus IX51 microscope. Scale bar: 100 μm. Results are represented as mean ± SEM of at least three independent experiments (****$p <$ 0.0001).

free phenformin on the human body induces severe side effects, such as lactic acidosis.[25] Therefore, we aimed to develop anti-CD147 liposomes carrying phenformin to specifically introduce this drug in highly CD147-expressed cancer cells and, in this way, reduce the side effects of phenformin. As a first approach, we tested the concentration at which liposomes would not be toxic for A549 and H292 cells. The results showed that at least up to 2 mM, liposomes did not have toxic effects to the cells (Figure S1c, Supporting Information). Therefore, we next evaluated the effect of 1 mM of LUVs carrying ≈500 μM of phenformin on A549, H292, and PC-9 cell viability by SRB assay. As shown in **Figure 5**a, liposomes carrying phenformin significantly decreased the cell viability of the three cell lines.

Following these results, we went to verify whether the amount of phenformin loaded in the nanocarriers was able to inhibit the oxidative phosphorylation (OXPHOS); and consequently, increase glycolytic flux and lactate production in A549 and H292 cells. The data showed that phenformin-loaded liposomes led to increased lactate production in both cell lines, suggesting that phenformin was, indeed, inhibiting the complex I of the respiratory chain and shifting cell metabolism to glycolysis (Figure S1d, Supporting Information). Regarding 3D-cell culture models, 1 mM of LUVs carrying 500 μM of phenformin was able to significantly decrease A549, H292, and PC-9 3D-spheroid growth (Figure 5b).

2.6. Internalization of Anti-CD147 LUVs

Upon optimization of the concentration of LUVs incorporating or not incorporating phenformin, anti-CD147 LUVs carrying phenformin were produced. In order to study whether the liposomes

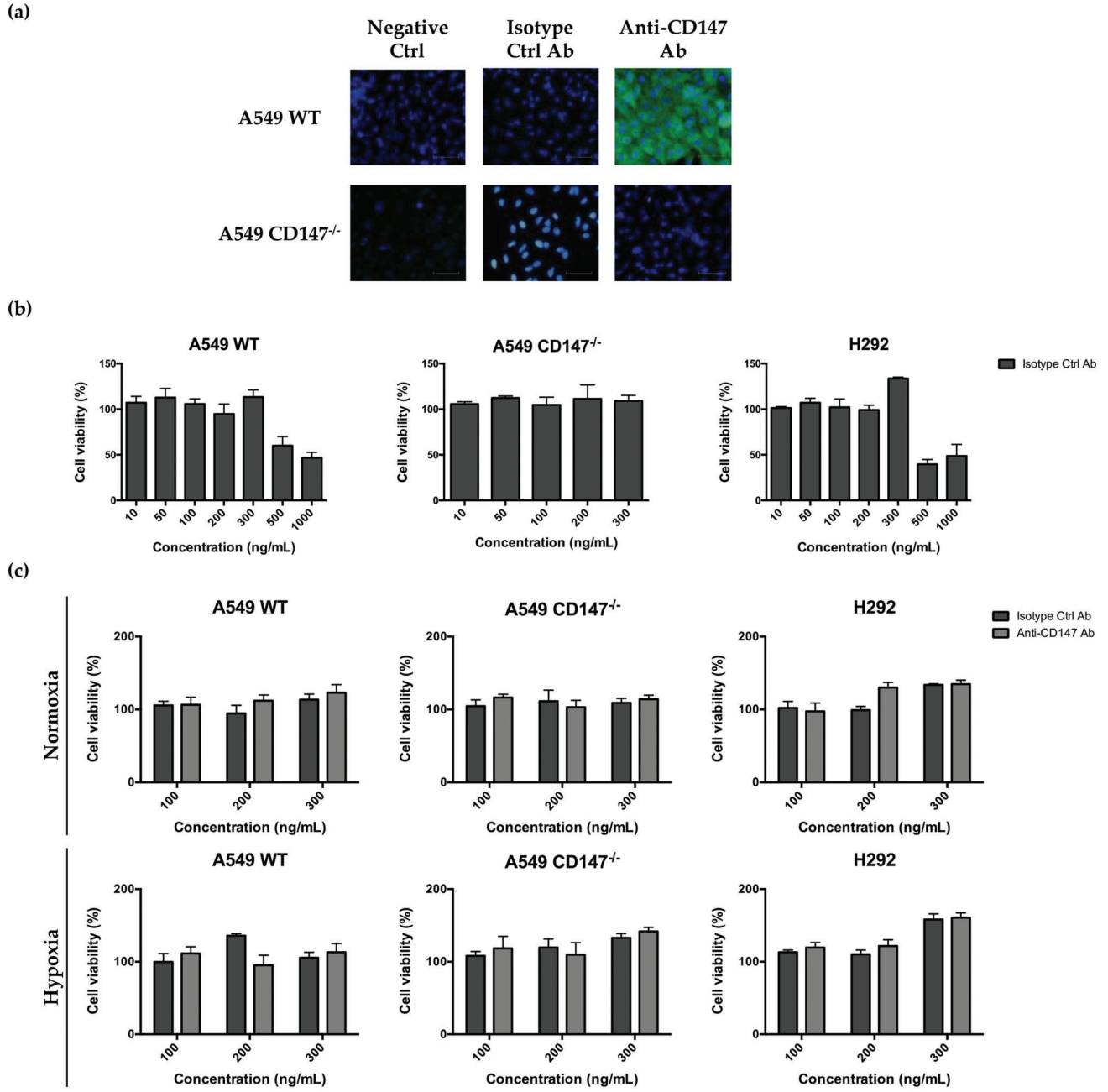

Figure 3. Anti-CD147 Ab effect on lung cancer cell viability. a) Immunofluorescence analysis of CD147 in A549 WT and A549 CD147KO$^{(-/-)}$ cells treated with the anti-CD147 Ab. 200× magnification (DAPI, blue – nuclei; Green – CD147). Scale bar: 50 μm. b) Increasing concentrations of Isotype Ctrl Ab (10–1000 ng mL^{-1}) and c) anti-CD147 Ab (100–300 ng mL^{-1}) were given to A549 WT, A549 CD147$^{-/-}$, and H292 cell lines, and cell viability was assessed by SRB assay after 24 h. Results are represented as mean ± SEM of at least three independent experiments.

would be able to permeate a tumor mass and enter into lung cancer cells, the generated A549 3D-spheroids were treated with 1 mM of anti-CD147 LUVs. After 10 days, we collected these spheroids for further immunofluorescence analysis. Using confocal microscopy, we confirmed that these nanocarriers internalized the 3D-spheroid tumor mass and reached the cytoplasm of A549 cells (green staining). The anti-CD147 Ab was retained at the cell surface of the peripheral cells of tumor spheroids (red staining) (**Figure 6**a).

2.7. Impact of Anti-CD147 LUVs Carrying Phenformin on Lung Cancer Cell Growth In Vitro

We next tested the impact of 1 mM of anti-CD147 LUVs carrying 500 μM of phenformin on 2D and 3D cancer cell growth of A549 and PC-9 cells. The results obtained demonstrated these nanocarriers were able to significantly decrease lung cancer cell viability (Figure 6b). Moreover, A549 and PC-9 3D-spheroid size was significantly reduced after 10 and 11 days of

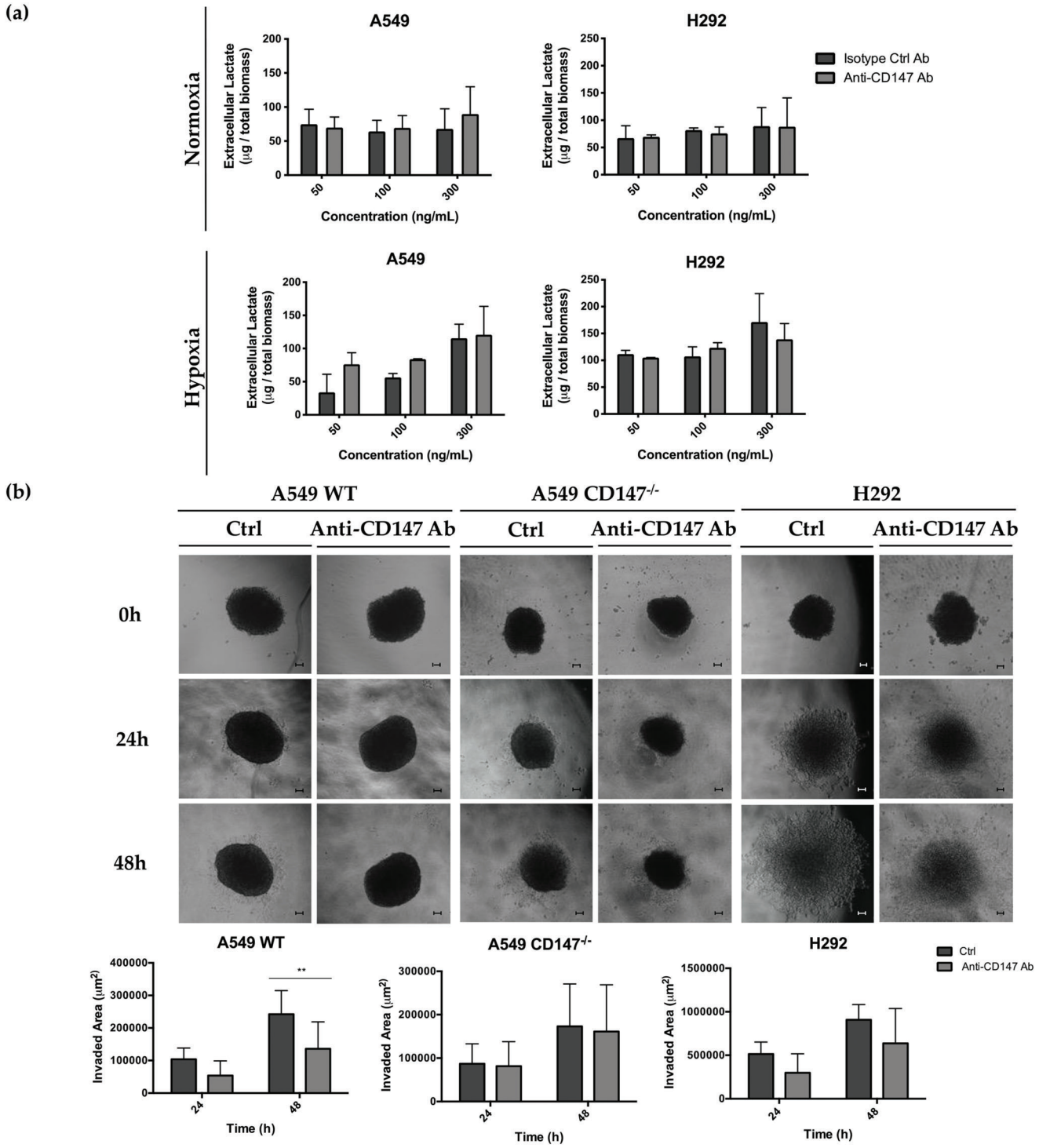

Figure 4. Anti-CD147 Ab effect on lung cancer cell metabolism and invasion. a) Extracellular lactate was quantified in A549 and H292 cells after 24 h of incubation with Isotype Ctrl and anti-CD147 antibodies (50–300 ng mL^{-1}) under normoxic or hypoxic conditions. Results were normalized for the total biomass. b) Cell invasion was assessed in A549 WT, A549 $CD147^{-/-}$, and H292 3D-spheroids after 24 and 48 h of incubation with and without 300 ng mL^{-1} anti-CD147 Ab ($n_{spheroids} = 5$ per condition). 40× magnification. Scale bar: 10 µm. Results are represented as mean ± SEM of at least three independent experiments (**$p < 0.01$).

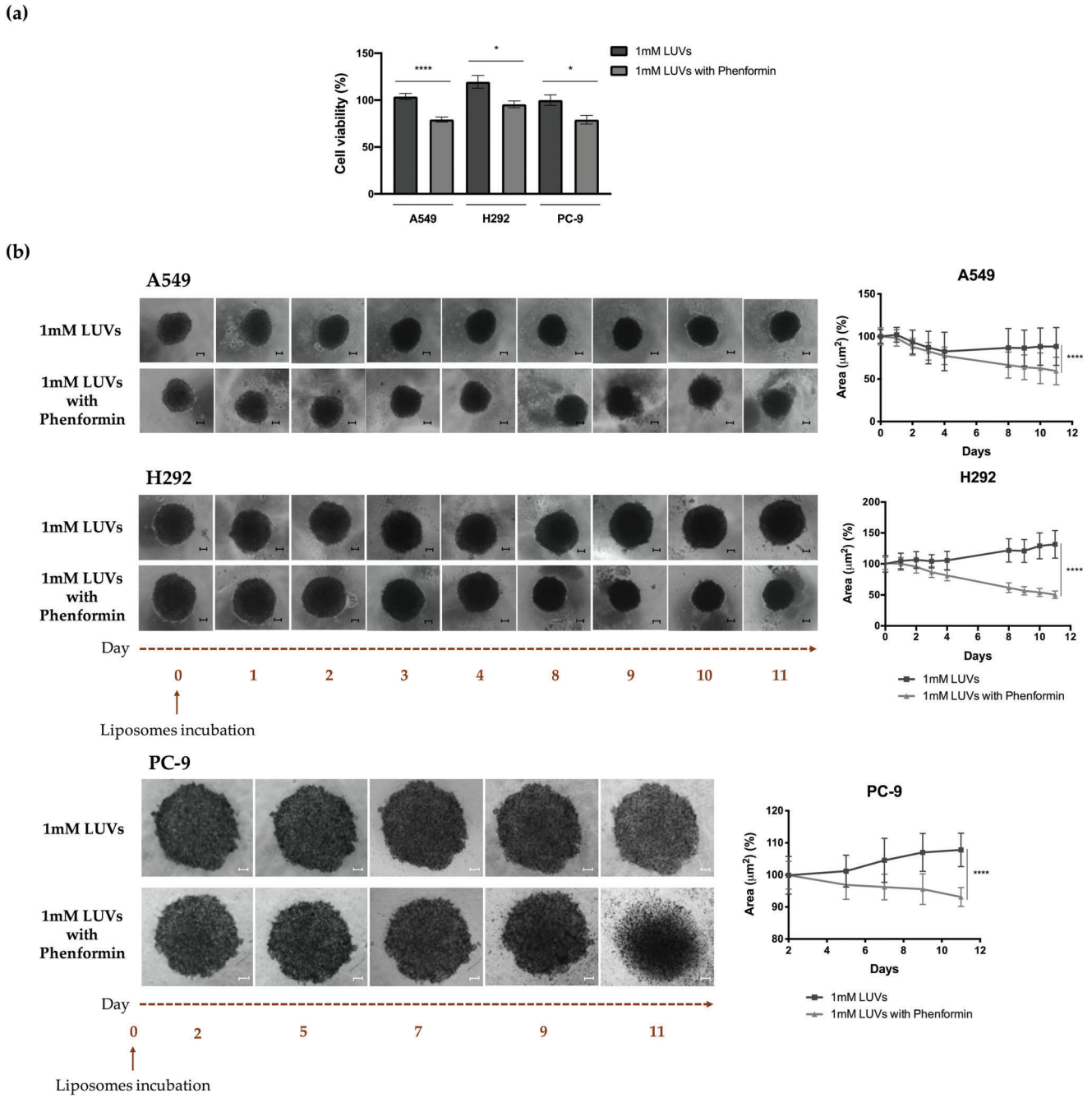

Figure 5. Effect of liposomes carrying phenformin on 2D and 3D-lung cancer cell growth. a) Cell viability after 24 h treatment with LUVs or LUVs carrying phenformin (500 μM). b) 3D-spheroids growth was analyzed after treatment with LUVs or LUVs carrying phenformin (500 μM) ($n_{spheroids}$ = 8 per condition). A549 and H292 3D-spheroid images were taken at 40× magnification (Scale bar: 100 μm) and PC-9-spheroids (Scale bar: 200 μm). Results are represented as mean ± SEM of at least three independent experiments (*$p < 0.05$; ****$p < 0.0001$).

Table 1. Size, PDI, and zeta-potential of LUVs incorporating or not incorporating phenformin.

Formulation	Size [nm]	PDI	Zeta-potential [mV]
LUVs	153.9 + 5.3	0.15 + 0.02	−23.6 + 3.7
LUVs + phenformin	158.4 + 8.1	0.18 + 0.01	−28.5 + 4.3

Values are reported as average ± SD of three independent measurements.

treatment with anti-CD147 LUVs with phenformin, respectively (Figure 6c).

2.8. In Vivo Anti-Cancer Efficacy of Anti-CD147 LUVs Carrying Phenformin

Last, the in vivo anti-cancer efficacy of anti-CD147 LUVs carrying phenformin was tested using the chicken embryo chorioallantoic

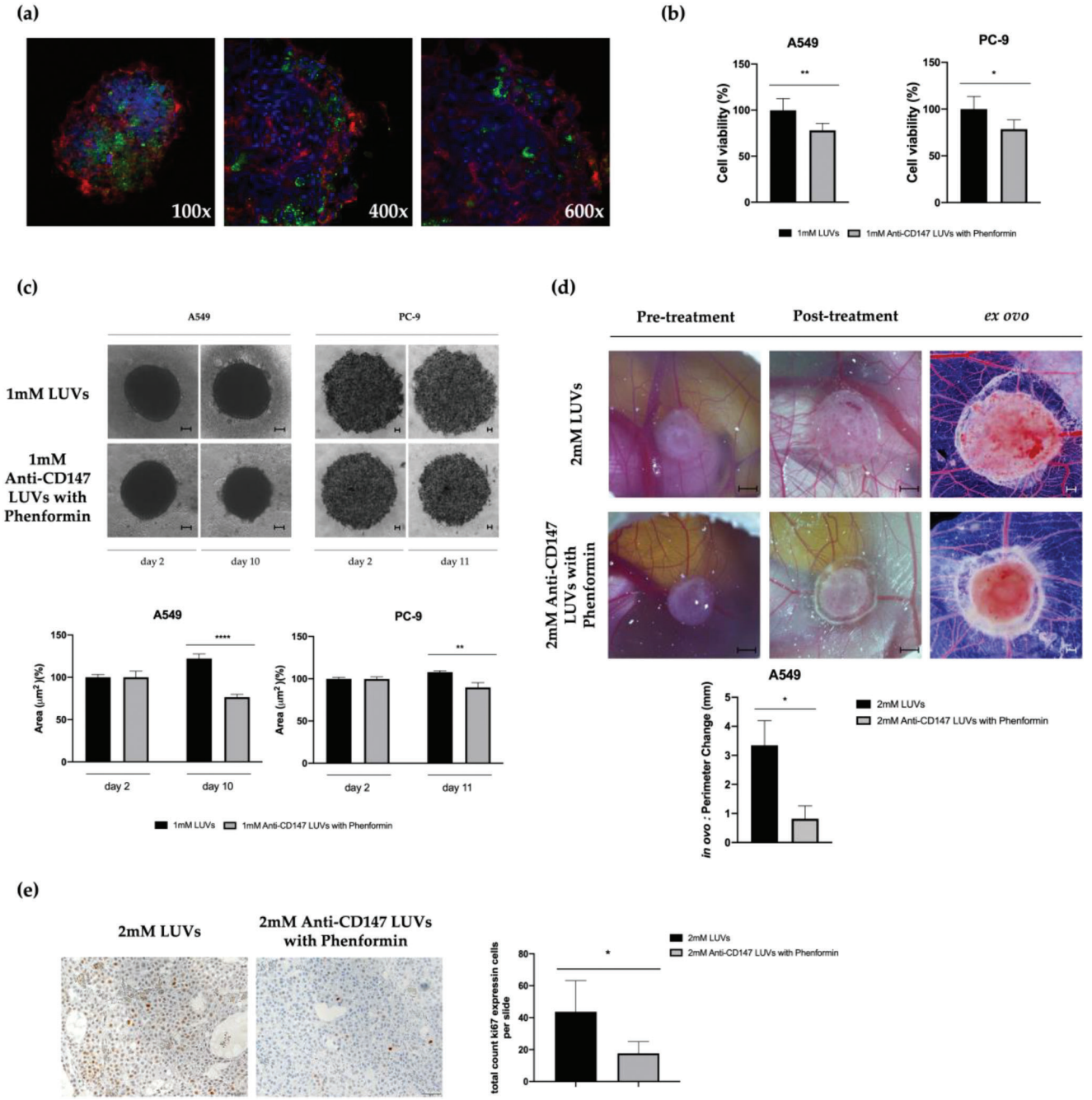

Figure 6. Internalization of Anti-CD147 LUVs with phenformin and their impact on lung cancer cell growth in vitro and in vivo. a) A549 3D-spheroids treated with 1 mM of anti-CD147 LUVs. Images were taken at the identified magnifications using the Olympus FLUOVIEW FV1000 confocal laser scanning microscope (DAPI, Blue – nuclei; NBD-cholesterol, Green – LUVs; Alexa Fluor 594, Red – anti-CD147 Ab). b) A549 and PC-9 cell viability upon treatment with LUVs or anti-CD147 LUVs carrying 500 µM of phenformin for 24 h. c) 3D-spheroid growth after treatment with LUVs or anti-CD147 LUVs carrying 500 µM of phenformin ($n_{spheroids}$ = 8 per condition). d) Anti-cancer effect of LUVs (n_{eggs} = 9) or anti-CD147 LUVs carrying 1000 µM of phenformin (n_{eggs} = 11) in A549 lung tumor growth. Representative images of CAMs were taken using a stereomicroscope, at day 13 and day 17 in ovo (Scale bar: 2 mm) and ex ovo (Scale bar: 1 mm). e) Representative pictures of Ki67 staining and the respective quantification of CAM tissues treated with 2 mM of LUVs or anti-CD147 LUVs carrying phenformin. Results are represented as mean ± SEM of at least three independent experiments (*$p < 0.05$; **$p < 0.01$; ****$p < 0.0001$).

membrane (CAM) model. The data showed no differences between vehicle and LUVs-treated groups (data not shown). Importantly, and as shown in Figure 6d, A549 lung tumors treated with 2 mM of anti-CD147 LUVs carrying 1000 μM phenformin presented lower tumor perimeters than LUVs-treated tumors. Moreover, the number of cells expressing Ki-67, a proliferation marker, significantly decreased in A549 lung tumors treated with 2 mM of anti-CD147 LUVs carrying 1000 μM phenformin when compared with the control group (Figure 6e).

3. Discussion

Lung cancer is the leading cause of cancer-related death worldwide.[26,27] Although the development of personalized therapies for specific molecular targets has helped to improve the survival of the patients, the overall 5-year survival rates remain poor.[28] Therefore, the search for new therapeutic targets and further advances in lung cancer treatments are needed.

Most cancers, including lung malignancies, are characterized by an exorbitant glycolytic phenotype to generate energy and metabolic intermediates, even under high oxygen tension.[29] This metabolic reprogramming was associated with tumor aggressiveness, namely acidity, invasion, and metastization.[30] Several therapies targeting the glycolytic pathway have already entered in clinical trials; however, the high plasticity of tumor cells remains a hindrance.[31] Therefore, it is crucial to develop potent anticancer drugs that will inhibit more than one bioenergetic pathway.

Recently, our group demonstrated that knockout of CD147 in lung cancer cell lines impaired the glycolytic metabolism and shifted cell metabolism into OXPHOS, which ultimately sensitized these cells to phenformin.[15] This drug belongs to the family of biguanides, a class of anti-diabetic drugs. The anti-tumor activity of these drugs has been already studied in several types of cancer. Phenformin has been found to possess more potent antitumor activities than metformin; however, the high incidence of lactate acidosis associated led to its discontinuation as a diabetic drug.[25,32]

In the last years, nanotechnology has gained increased attention and several nanocarriers were approved or are undergoing clinical trials for cancer treatment, including lung cancer.[33,34] Within nanocarriers, liposomes have been the most widely applied clinically, owing to their size, biodegradable, and biocompatible composition.[4,35] Several reports have suggested that by incorporating the desired chemotherapeutic agent into liposomes functionalized with tumor-targeting ligands, the adverse effects of conventional chemotherapeutics can be substantially ameliorated, and the intracellular uptake is increased.[36–38]

In this regard, we hypothesized that formulating phenformin into liposomes would enhance its anti-cancer effect and reduce its off-target effects. In order to augment their selectivity to tumor cells and avoid a systemic effect of phenformin, liposomes were functionalized with antibodies against CD147, a biomarker of several tumors.[39–41] Besides that, with these immunoliposomes, we intended to inhibit CD147 function. Therefore, we designed and created a new therapeutic approach based on anti-CD147 liposomes carrying phenformin to target lung cancer.

Before the development and evaluation of the efficacy of functionalized anti-CD147 liposomes carrying phenformin on lung cancer cells, we characterized the anti-tumor effect of phenformin and anti-CD147 Ab (i.e., Leaf Purified Anti-Human CD147 antibody). First, we investigated whether the lung cancer cells respond to phenformin.[42] As we previously reported, all cell lines exhibited high sensitivity to phenformin in a dose-dependent manner.[32] Moreover, the IC_{50} values indicated that H292 cells were slightly more sensitive to this biguanide drug than A549 and PC-9 cells. A possible explanation for these results is the fact that H292 cell metabolism could also rely on glutaminolysis because it was reported that these cells present higher glutaminase activity, a metabolic enzyme which catalyzes the conversion of glutamine into glutamate and ammonia.[43] Indeed, it was described that cancer cells have a heavy demand for glutamine amino-acid.[44]

To validate the anti-cancer effect of phenformin, we evaluated its effect on A549, H292, and PC-9 3D-spheroid growth. Similar to the 2D-cell culture studies, the results showed a significant decrease in tumor-spheroid size throughout the time. These findings demonstrated that phenformin could be a suitable drug to be included in nanoparticles because it showed a potent effect against lung cancer cells.

Next, we assessed whether the anti-CD147 Ab could specifically target and inhibit CD147 protein at the surface of lung cancer cells. The data confirmed that this antibody is specific for CD147-expressing cancer cells; however, no effects were found in A549 and H292 cell viability and metabolism. These findings suggest that this antibody does not interrupt the interaction between CD147 and MCTs; and consequently, does not compromise their activity. Besides its role as MCT chaperone, CD147 interacts with different molecules playing a role in various physiological and pathological processes, such as cell remodeling and invasion.[45] Indeed, it is known that the interaction of CD147 with integrins mediates cell migration and invasion.[46] Furthermore, CD147 enhances the production of MMPs and the major constituent of the extracellular matrix, hyaluronan, in order to assist cell migration and invasion.[41,47,48] Bearing this in mind, we decided to study the effect of anti-CD147 Ab on lung cancer cell invasion. Indeed, a significant reduction in the invasiveness capacity of A549 WT cells was observed, contrarily to A549 CD147KO cells. Although we did not find significant differences for H292 cells, it was possible to observe a trend decrease in cell invasion for this cell line. These data are in accordance with the Amit–Choen et al. investigation, in which they demonstrated that the Leaf Purified Anti-Human CD147 antibody was able to decrease the MMP-9 secretion in co-cultures of renal and breast carcinoma cell lines with monocytic-like cell lines, suggesting that it is able to diminish cancer cell invasion.[49]

The adverse effects of conventional chemotherapeutics can be substantially ameliorated by incorporating the desired chemotherapeutic agent inside nanocarriers. In this regard, we hypothesized that incorporating phenformin into liposomes would enhance its anti-cancer effect and reduce its toxic effects, particularly in the liver. As mentioned before, these side effects are attributed to the fact that phenformin crosses biological membranes by passive diffusion, contrarily to other biguanides that require active transporters.[20] Although drug-loaded liposomes have already achieved significant advances, the anti-tumor effect of a chemotherapeutic agent can be enhanced by ligand-mediated targeting.[33]

In this sense, we coated liposomes with anti-CD147 antibodies in order to augment their selectivity to CD147-expressing cancer cells and avoid a systemic effect of phenformin. Besides that, with these immunoliposomes, we intended to impair CD147 function. Actually, some researchers have tried to construct CD147 antibody-conjugated immunoliposomes in order to enhance selective drug delivery to tumor cells. For instance, Asakura and its collaborators constructed anti-CD147-labeled polymeric micelles to encapsulate a conjugate of doxorubicin with glutathione and they found a specific accumulation of anti-CD147 micelles in CD147-expressing cells. Besides that, the cell death rate for anti-CD147 micelles was ≈threefold higher than for the IgG micelles.[50] Wang et al. developed CD147-targeted doxorubicin-loaded immunoliposomes and they verified these nanocarriers were able to deliver doxorubicin to CD147-overexpressing cancer cells specifically in vitro and in vivo with higher efficacy than the non-targeted controls.[38]

Herein, we started by preparing and investigating the anti-cancer effect of LUVs carrying phenformin on lung cancer cell behavior. Interestingly, we observed that liposomes carrying phenformin significantly decreased 2D and 3D-A549, H292 and PC-9 cell growth, without toxic effects. Importantly, we confirmed liposome internalization by confocal microscopy, and we observed a significantly reduction in A549 and PC-9 3D-spheroid size throughout the time. Last, we validated the anti-cancer efficacy of anti-CD147 liposomes carrying phenformin in vivo using the CAM model. This is a useful technique for early pre-clinic in vivo efficacy studies of potential anti-cancer treatments due to the rapid development of the chick embryo and easy accessibility to the CAM. In addition, the immunodeficiency of the host during the first 18 days of development allows the implantation of tumor cells without triggering an immune response. In addition, this model has ethical advantages in comparison to several mammalian in vivo models because it does not require ethics committee approval for animal experimentation: the chick embryo is unable to experience pain. Last, CAM successfully supports most cancer cell characteristics including growth, invasion, angiogenesis, and remodeling of the microenvironment being an attractive option for in vivo experiments in early pre-clinical studies.[51] Herein, this model was used to demonstrate a significant reduction of A549 tumor growth in CAMs treated with anti-CD147 liposomes carrying phenformin, compared to control. Furthermore, this treatment led to a decrease in Ki-67 proliferating cells, with no observation of toxicity-associated alterations in the chicken embryos.

4. Conclusion

In this study, homogeneous populations of anti-CD147 LUVs carrying phenformin were developed to successfully decrease CD147-overexpressing tumor cell growth. In summary, we demonstrated the therapeutic relevance of both phenformin and anti-CD147 Ab in a series of cancer cell behavior assays. Then, we validated the efficacy of CD147-targeted liposomes carrying phenformin by presenting strong evidence that they have a potent anti-cancer effect in CD147-positive cells. Herein, we expect to reveal a novel strategy to target tumor metabolism and provide an effective therapy for lung cancer.

5. Experimental Section

Reagents: 1,2-dipalmitoyl-sn-glycero-3-phosphocholine (DPPC) and 1,2-distearoyl-sn-glycero-3-phosphoethanolamine-*N* [maleimide(polyethyleneglycol)-2000] (ammonium salt) (DSPE-PEG (2000)-Maleimide) were purchased from Avanti Polar Lipids. Cholesterol, HEPES hemisodium salt, 2-iminothiolane (2IT), ethylenediaminetetraacetic acid (EDTA), and phosphate buffered saline (PBS) tablets were purchased from Sigma–Aldrich. 22-(*N*-(7-nitrobenz-2-oxa-1,3-diazol-4-yl) amino)-23,24-bisnor-5-cholen-3ß-ol (NBD cholesterol) was acquired from Thermo Fisher Scientific.

The monoclonal Leaf Purified Anti-Human CD147 (ref. 306206 – Biolegend) and Leaf Purified Mouse IgG1, k Isotype Ctrl antibodies (ref. 400124 – Biolegend) were reconstituted at a stock concentration of 2 µg mL^{-1} in sterile PBS 1×. Phenformin hydrochloride (Sigma–Aldrich) was diluted in sterile water to 200 mM stock solution. Working concentrations were obtained by diluting these drugs in culture medium. Cell culture medium was used as control (vehicle).

Cell Lines and Cell Culture: The human lung adenocarcinoma A549 and PC-9 and the mucoepidermoid pulmonary H292 cell lines were purchased from American Type Culture Collection (ATCC, Manassas, VA). A549 cell line was previously knocked-out for CD147.[52] All cell lines were maintained in Dulbecco's modified Eagle medium (DMEM) supplemented with 10% of fetal bovine serum (FBS) (Biochrom, Merck) and 1% of penicillin/streptomycin (Gibco, Life Tecnologies Corporation). For normoxic conditions, cells were incubated in a humidified atmosphere of 21% O_2, 5% CO_2, and 74% N_2 at 37 °C. For induction of hypoxia, cells were placed in an airtight chamber with a hypoxic gas mixture of 1% O_2, 5% CO_2, and 95% N_2 and incubated at 37 °C. Oxygen levels were monitored using an oxygen sensor.

Liposome Preparation and Characterization: Large unilamellar liposomes (LUVs) were produced according to the thin film hydration method followed by extrusion.[53,54] Briefly, the lipid film composed of DPPC/DSPE-PEG-Mal/cholesterol (molar ratio of 1.85:0.15:1) or DPPC/DSPE-PEG-Mal/cholesterol/NBD cholesterol (to enable the evaluation of LUVs internalization; molar ratio of 1.85:0.15: 0.82:0.18) was formed after complete organic solvents evaporation in a rotary evaporator (RV10 AUTO, IKA). The hydration of the dried lipid film was performed with HEPES buffer (pH 7.4, 10 mM) or with a HEPES buffered solution of phenformin at ≈42 °C. The resulting mixture in the presence of glass beads was vortexed to produce multilamellar liposomes (MLVs). Afterward, MLVs were extruded at ≈42 °C using an Avanti Mini-Extruder, forty-three times through polycarbonate filters of 0.1 µm pore diameter, to originate LUVs.

For LUVs functionalization, first anti-CD147 antibodies were thiolated by their incubation with a 100-fold molar excess of 2IT in the presence of 5 mM EDTA (to avoid the oxidation of thiol groups) in PBS (pH 8.0) for 1 h at room temperature (RT).[55] Then, a dialysis (Micro Float-A-Lyzer, MWCO: 3.5-5 kDa) was performed to remove the excess of 2IT. As thiol groups have a rapid rate of recyclization, the buffer replacement was performed each 15–20 min during a period of time less than 4 h.[55,56] Then, the thiolated anti-CD147 antibodies were incubated overnight at 4 °C with LUVs. Exceeding this period of time, free antibodies were removed by washing LUVs twice with HEPES buffer using Vivaspin 300 kDa Filter Units (Fisher Scientific). This procedure was also performed to eliminate the non-encapsulated phenformin. The concentration of phenformin entrapped into LUVs was evaluated after liposomes dissolution in ethanol (dilution factor equal to or greater than 2.5). The absorbance of the resulting solution was measured at 236 nm using Standard UV–vis photospectrometry equipment (UV-1601, Shimadzu). The concentration of liposomes and phenformin was adjusted to obtain in 1 or 2 mM of phospholipids and 500 or 1000 µM. The quantitative determination of phospholipids was performed using the Bartlett method.[57,58] The absorbance of the blue colored complex was acquired at 830 nm using a microplate reader (Synergy HT, BioTek). The size, polydispersity index (PDI), and zeta-potential of LUVs suspensions (500 µM phospholipids) were assessed using dynamic light scattering (DLS) and laser Doppler microelectrophoresis, respectively, at 37.0 °C ± 0.1 °C. Disposable polystyrene

cuvettes and a dip cell were used to perform DLS and zeta-potential determinations, respectively, in a Zetasizer Nano ZS equipment (Malvern Instruments).

Western Blot: Approximately, 1×10^6 A549 WT, A549 CD147$^{-/-}$, and H292 were seeded per standard T25cm^2 flask and allowed to adhere overnight. Cells were incubated in normoxic or hypoxic conditions for 24 h. Afterward, cells were homogenized in lysis buffer with protease/phosphatase inhibitors (Roche) for 15 min; and then, centrifuged at 13 000 rpm for 15 min at 4 °C. The supernatants were collected and total protein was quantified using the Bradford method (Sigma). Western blot was performed as previously described by the authors' group.[59] Membranes were incubated overnight at 4 °C with the following primary antibodies: anti-CD147 (1:500, ref: 306202, Biolegend), anti-MCT1 (1:500, ref: sc-365501, Santa Cruz Biotechnology), anti-MCT4 (1:300, ref: sc-376465, Santa Cruz Biotechnology), and anti- β-Actin (ref: 1:50, sc-8432, Santa Cruz Biotechnology). Afterward, membranes were incubated with a goat anti-mouse IgG-HRP secondary antibody (1:5000, ref: sc-2031, Santa Cruz Biotechnology) for 1 h at RT. Bound antibodies were visualized by chemiluminescence (SuperSignal West Femto kit, Thermo Scientific). β-Actin was used as loading control.

Immunofluorescence: A549 WT and CD147$^{-/-}$ (8×10^4/well) and H292 cells (5×10^4/well) were seeded on glass coverslips placed into 12-well plates and allowed to adhere overnight. After 24 h in normoxic or hypoxic conditions, cells were fixed and permeabilized with cold methanol during 20 min at RT; and then, blocked with 5% of bovine serum albumin (BSA) for 30 min. Slides were incubated overnight at RT with the following primary antibodies: anti-CD147 (1:400, ref: 306202, Biolegend), anti-MCT1 (1:400, ref: ab3538P, Chemicon), anti-MCT4 (1:400, ref: sc-376465, Santa Cruz Biotechnology), and Purified Mouse IgG1, k Isotype Ctrl antibodies (1:400, ref: 400 124, Biolegend) diluted in 5% BSA. After washing, slides were incubated for 1 h at RT with the following secondary antibodies: Alexa Fluor 594 goat anti-mouse (ref: A11032), Alexa Fluor 488 goat anti-mouse (ref: A11001), and Alexa Fluor 568 goat anti-rabbit (ref: A11011) (1:400, Life Technologies). Nuclei were stained with DAPI and images were obtained with a fluorescent microscope (Olympus BX16), using the Cell P software.

Cell Viability Assay: Cells were plated at an initial concentration of 8×10^3 (A549 WT and CD147$^{-/-}$), 1×10^3 (PC-9), or 5×10^3 (H292) per well into 96-well plates and allowed to adhere overnight. Cells were incubated in DMEM 1% FBS without or with phenformin (0.01-4 mM), isotype ctrl (10–1000 ng mL^{-1}), and anti-CD147 antibodies (100–300 ng mL^{-1}) or with LUVs (1–8 mM) and LUVs carrying phenformin (1 mM). After 24, 48, or 72 h of incubation, cell viability was evaluated through the Sulforhodamine B Assay (SRB; TOX-6, Sigma–Aldrich) according to the manufacturer's instructions and as previously described.[59] All results were normalized to the respective controls.

Extracellular Lactate Measurements: A549 and H292 were seeded in 48-well plates at a density of 1.2×10^4 and 1×10^4 cells per well, respectively, and allowed to adhere overnight. Cells were incubated with DMEM 10% FBS supplemented with isotype ctrl/anti-CD147 antibodies (50–300 ng mL^{-1}) or with LUVs carrying or not phenformin (1 mM) under normoxic and hypoxic conditions for 24 h. Lactate content was analyzed in the cell culture supernatant using a commercial kit (Spinreact), as previously described.[59] Results were expressed as total µg per total biomass. Total biomass was assessed through the SRB assay.

3D Cultures: Single cell suspensions of 5×10^3 A549 and H292 cells were seeded per well on agarose-coated 48-well plates. PC-9 (4×10^3) cell suspensions were placed in poly-2-hydroxyethylmethacrylate (poly-HEMA) coated U-bottom 96-well plates. Plates were centrifuged at 1200 rpm for 10 min and incubated in a 37 °C, 5% CO_2 incubator. After 5 days, spheroids were incubated with DMEM 10% FBS without or with phenformin (1–2 mM), LUVs carrying or not carrying phenformin (1 mM) or anti-CD147 LUVs carrying phenformin (1 mM) diluted in DMEM 10%FBS. Spheroid morphology was observed along time and images were collected using the Olympus IX51 microscope or the Olympus S2916 stereomicroscope equipped with a digital camera (Olympus DP71). Tumor spheroid area was determined using the ImageJ software. For the internalization studies, an immunofluorescence analysis was performed after 10 days of treatment and images were taken at the Olympus FLUOVIEW FV1000 confocal laser scanning microscope.

Cell Invasion Assay: This assay was performed using spheroids prepared as previously mentioned. After 5 days, spheroids were transferred into 96-well plates and incubated with 300 ng mL^{-1} of anti-CD147 Ab diluted in matrigel. Spheroid morphology was observed along time and images were collected using the Olympus IX51 microscope. The spheroids area and spheroids invaded area were determined using the ImageJ software.

Chicken Chorioallantoic Membrane (CAM) Assay: CAM assay was performed as previously described.[60] Briefly, on the 9th day of embryo development, 2×10^6 of A549 cells (in 10 µL of matrigel) were injected into the CAM. After 4 days, tumors were treated with the vehicle (DMEM 10%FBS), 2 mM of LUVs or 2 mM of anti-CD147 LUVs carrying 1000 µM of phenformin. At day 17 of embryo development (endpoint), only live embryos/eggs were included in the analysis. There was no apparent embryo toxicity as a result of the tumor implantation procedure. Tumors were photographed in ovo using the Olympus S2916 stereomicroscope equipped with a digital camera (Olympus DP71). CAMs and tumors were dissected, fixed in 3.7% paraformaldehyde, and photographed ex ovo. Tumor perimeter was measured using the Image J software.

Immunohistochemistry: Histological slides of A549 tumors implanted on CAMs were subjected to immunohistochemistry using a polymer system (UltraVision ONE Detection System: HRP Polymer Lab Vision Corporation, Fremont, Ca.). Briefly, deparaffinized and rehydrated slides were incubated with 10 mM citrate buffer (pH 6.0) for 15 min in a microwave at 600 W for antigen retrieval. Then, the sections were incubated overnight at RT with a primary anti-Ki-67 antibody (1:100, ref: 350501 Biolegend). The immune reaction was visualized using 3,3'-Diamonobenzidine (DAB, UltraVision Quanto HRP) as chromogen, and tumor tissue sections were counterstained with hematoxylin. Stained slides were evaluated and photographed using a bright field microscope Olympus BX61. The number of Ki-67 positive cells was counted based on four different images from the same slide.

Statistical Analysis: Results are expressed as the mean ± standard error of the mean (SEM) of at least three independent experiments. Normality and homoscedasticity were evaluated with Shapiro-Wilk's and Levene's tests, respectively. An unpaired or paired-sample *t*-test was carried out to analyze differences between unrelated or related groups, respectively, and for multiple comparison analyzes, a two-way ANOVA post-hoc Sidak's test was applied. All analyses were performed with GraphPad Prism (GraphPad Prism software, Inc., version 6), and statistically significant differences were considered when *p*-values were lower than 0.05.

Supporting Information

Supporting Information is available from the Wiley Online Library or from the author.

Acknowledgements

This work was supported by the Fundação para a Ciência e a Tecnologia (FCT) – project UIDB/50026/2020 and UIDP/50026/2020 and by the project NORTE-01-0145-FEDER-000055 supported by Norte Portugal Regional Operational Programme (NORTE 2020), under the PORTUGAL 2020Partnership Agreement, through the European Regional Development Fund (ERDF). S.G. and A.P.-N. received fellowships from FCT (SFRH/BPD/117858/2016 and SFRH/BD/148476/2019, respectively).

Conflict of Interest

The authors declare no conflict of interest.

Author Contributions

A.P.-N., H.F., S.A., M.G., and S.G. conducted most of the experiments and analyzed the results. A.P.-N. and S.G. wrote the paper. H.F., N.M.N., F.B.,

and S.G. conceived, designed, and analyzed the results. H.F. and S.G. coordinated the project. All authors reviewed the results and approved the final version of the manuscript.

Data Availability Statement

The data that support the findings of this study are available from the corresponding author upon reasonable request.

Keywords

CD147, liposomes, lung cancer, phenformin

Received: February 16, 2023
Revised: April 26, 2023
Published online: June 11, 2023

[1] H. Sung, J. Ferlay, R. L. Siegel, M. Laversanne, I. Soerjomataram, A. Jemal, F. Bray, *CA Cancer J. Clin.* **2021**, *71*, 209.
[2] A. A. Thai, B. J. Solomon, L. V. Sequist, J. F. Gainor, R. S. Heist, *Lancet* **2021**, *398*, 535.
[3] C. Zhang, N. B. Leighl, Y. L. Wu, W. Z. Zhong, *J. Hematol. Oncol.* **2019**, *12*, 45.
[4] A. Akbarzadeh, R. Rezaei-Sadabady, S. Davaran, S. W. Joo, N. Zarghami, Y. Hanifehpour, M. Samiei, M. Kouhi, K. Nejati-Koshki, *Nanoscale Res. Lett.* **2013**, *8*, 102.
[5] F. U. Din, W. Aman, I. Ullah, O. S. Qureshi, O. Mustapha, S. Shafique, A. Zeb, *Int. J. Nanomedicine* **2017**, *12*, 7291.
[6] B. Romberg, W. E. Hennink, G. Storm, *Pharm. Res.* **2008**, *25*, 55.
[7] J. Gao, H. Chen, H. Song, X. Su, F. Niu, W. Li, B. Li, J. Dai, H. Wang, Y. Guo, *Mini Rev. Med. Chem.* **2013**, *13*, 2026.
[8] L. Xiong, C. K. Edwards 3rd, L. Zhou, *Int. J. Mol. Sci.* **2014**, *15*, 17411.
[9] A. Landras, C. Reger de Moura, F. Jouenne, C. Lebbe, S. Menashi, S. Mourah, *Cancers* **2019**, *11*, 1803.
[10] Y. H. Kuang, Y. J. Liu, L. L. Tang, S. M. Wang, G. J. Yan, L. Q. Liao, *Hong Kong Med. J.* **2018**, *24*, 252.
[11] F. Peng, H. Li, Q. You, H. Li, D. Wu, C. Jiang, G. Deng, Y. Li, Y. Li, Y. Wu, *Biomed Res. Int.* **2017**, *2017*, 5019367.
[12] M. S. Ullah, A. J. Davies, A. P. Halestrap, *J. Biol. Chem.* **2006**, *281*, 9030.
[13] V. Miranda-Gonçalves, S. Granja, O. Martinho, M. Honavar, M. Pojo, B. M. Costa, M. M. Pires, C. Pinheiro, M. Cordeiro, G. Bebiano, P. Costa, R. M. Reis, F. Baltazar, *OncoTargets Ther.* **2016**, *7*, 46335.
[14] X. Ke, F. Fei, Y. Chen, L. Xu, Z. Zhang, Q. Huang, H. Zhang, H. Yang, Z. Chen, J. Xing, *Carcinogenesis* **2012**, *33*, 1598.
[15] S. Granja, I. Marchiq, R. Le Floch, C. S. Moura, F. Baltazar, J. Pouysségur, *OncoTargets Ther.* **2015**, *6*, 6708.
[16] K. J. Mc, K. Kuwayti, P. P. Rado, *Can. Med. Assoc. J.* **1959**, *80*, 773.
[17] M. E. McGuinness, R. L. Talbert, *Ann. Pharmacother.* **1993**, *27*, 1183.
[18] H. R. Bridges, V. A. Sirviö, A.-n.A. Agip, J. Hirst, *BMC Biol.* **2016**, *14*, 65.
[19] A. L. Jackson, W. Sun, J. Kilgore, H. Guo, Z. Fang, Y. Yin, H. M. Jones, T. P. Gilliam, C. Zhou, V. L. Bae-Jump, *OncoTargets Ther.* **2017**, *8*, 100113.
[20] M. Pollak, *J. Clin. Invest.* **2013**, *123*, 3693.
[21] H. R. Bridges, V. A. Sirviö, A.-N. A. Agip, J. Hirst, *BMC Biol.* **2016**, *14*, 65.
[22] M. Eugenia, E. Carrillo, G. Ruiz, A. Dom, J. A. Marchal, H. Boulaiz, *Int. J. Mol. Sci.* **2019**, *20*, 3316.
[23] Z. Zhou, N. Jiang, J. Chen, C. Zheng, Y. Guo, R. Ye, R. Qi, J. Shen, *J. Nanobiotechnol.* **2021**, *19*, 375.
[24] B. Pinto, A. C. Henriques, P. M. A. Silva, H. Bousbaa, *Pharmaceutics* **2020**, *12*, 1186.
[25] H. Zhao, K. D. Swanson, B. Zheng, *Trends Cancer* **2021**, *7*, 714.
[26] F. Bray, J. Ferlay, I. Soerjomataram, R. L. Siegel, L. A. Torre, A. Jemal, *Ca-Cancer J. Clin.* **2018**, *68*, 394.
[27] J. Didkowska, U. Wojciechowska, M. Manczuk, J. Lobaszewski, *Ann. Transl. Med.* **2016**, *4*, 150.
[28] R. L. Siegel, K. D. Miller, A. Jemal, *Ca-Cancer J. Clin.* **2019**, *69*, 7.
[29] R. A. Gatenby, R. J. Gillies, *Nat. Rev. Cancer* **2004**, *4*, 891.
[30] A. Ibrahim-hashim, K. Bailey, Y. Balagurunathan, M. Jennifer, *Cancer Res.* **2014**, *73*, 1524.
[31] G. Kroemer, J. Pouyssegur, *Cancer Cell* **2008**, *13*, 472,.
[32] W. Xiong, L. Qi, N. Jiang, Q. Zhao, L. Chen, X. Jiang, Y. Li, Z. Zhou, J. Shen, *ACS Appl. Mater. Interfaces* **2021**, *13*, 8026.
[33] M. Zhao, Y. Sun, X. Zhu, D. Chen, S. Feng, S. Guo, W. Li, *Mini-Reviews in Medical Chemistry* **2016**, *13*, 2026.
[34] P. P. Deshpande, S. Biswas, V. P. Torchilin, *Nanomedicine* **2013**, *8*, 1509.
[35] S. Meng, B. Su, W. Li, Y. Ding, L. Tang, W. Zhou, Y. Song, Z. Caicun, *Med. Oncol.* **2011**, *28*, 1180.
[36] S. Krishnamurthy, V. W. L. Ng, S. Gao, M.S-h. Tan, Y. Y. Yang, *Biomaterials* **2014**, *35*, 9177.
[37] J. Wang, Z. Wu, G. Pan, J. Ni, F. Xie, B. Jiang, L. Wei, J. Gao, W. Zhou, *Nanomedicine* **2018**, *14*, 1949.
[38] R. Zhu, C.-g. Zhang, Y. Liu, Z.-q. Yuan, W.-l. Chen, S.-d. Yang, J.-z. Li, W.-j. Zhu, X.-f. Zhou, B.-g. You, X.-n. Zhang, *Sci. Rep.* **2015**, *5*, 17904.
[39] X. Kong, Y. Wang, C. Dai, W. Ma, R. Wang, *Mol. Neurobiol.* **2017**, *54*, 1568.
[40] X. Zhang, T. Tian, X. Zhang, C. Liu, X. Fang, *Oncotarget* **2017**, *8*, 37673.
[41] T. Zhang, H. Li, Y. Zhang, P. Wang, H. Bian, Z. N. Chen, *Oncol. Lett.* **2017**, *15*, 3042.
[42] M. R. Owen, E. Doran, A. P. Halestrap, *Biochem. J.* **2000**, *348*, 607.
[43] T. Han, W. Zhan, M. Gan, F. Liu, B. Yu, Y. E. Chin, J.-b. Wang, *Cell Res.* **2018**, *28*, 655.
[44] R. J. DeBerardinis, T. Cheng, *Oncogene* **2010**, *29*, 313.
[45] U. H. Weidle, W. Scheuer, D. Eggle, S. Klostermann, H. Stockinger, *Cancer Genomics Proteomics* **2010**, *7*, 157.
[46] E. E. Gabison, T. Hoang-Xuan, A. Mauviel, S. Menashi, *Biochimie* **2005**, *87*, 361.
[47] T. Muramatsu, *J. Biochem.* **2016**, *159*, 481.
[48] G. D. Grass, L. B. Tolliver, M. Bratoeva, B. P. Toole, *J. Biol. Chem.* **2013**, *288*, 26089.
[49] B.-C. Amit-Cohen, M. M. Rahat, M. A. Rahat, *Front. Physiol.* **2013**, *4*, 178.
[50] T. Asakura, M. Yokoyama, K. Shiraishi, K. Aoki, K. Ohkawa, *Anticancer Res.* **2018**, *38*, 1311.
[51] D. Ribatti, *Reprod. Toxicol.* **2017**, *70*, 97.
[52] S. Granja, I. Marchiq, R. Le Floch, C. S. Moura, F. Baltazar, J. Pouysségur, *OncoTargets Ther.* **2015**, *6*, 6708.
[53] A. D. Bangham, R. W. Horne, *J. Mol. Biol.* **1964**, *8*, 660.
[54] H. Ferreira, V. M. F. Gonçalves, R. Silva, M. E. Tiritan, M. Teixeira, A. Cavaco-Paulo, *Pharmacol. Pharm. Pharmacovigilance* **2017**, *1*.
[55] H. Kouchakzadeh, S. A. Shojaosadati, F. Tahmasebi, F. Shokri, *Int. J. Pharm.* **2013**, *447*, 62.
[56] L. Deng, Y. Zhang, L. Ma, X. Jing, X. Ke, J. Lian, Q. Zhao, B. Yan, J. Zhang, J. Yao, J. Chen, *Int. J. Nanomed.* **2013**, *8*, 3271.
[57] G. R. Bartlett, *J. Biol. Chem.* **1959**, *234*, 466.
[58] N. Monteiro, D. Ribeiro, A. Martins, S. Faria, N. A. Fonseca, J. N. Moreira, R. L. Reis, N. M. Neves, *ACS Nano* **2014**, *8*, 8082.
[59] F. Morais-Santos, S. Granja, V. Miranda-Gonçalves, A. H. J. Moreira, S. Queirós, J. L. Vilaça, F. C. Schmitt, A. Longatto-Filho, J. Paredes, F. Baltazar, C. Pinheiro, *OncoTargets Ther.* **2015**, *6*, 19177.
[60] V. Miranda-Gonçalves, M. Honavar, C. Pinheiro, O. Martinho, M. M. Pires, C. Pinheiro, M. Cordeiro, G. Bebiano, P. Costa, I. Palmeirim, R. M. Reis, F. Baltazar, *Neuro-Oncol.* **2013**, *15*, 172.

